Development 133, 3075-3083 (2006) doi:10.1242/dev.02473

Axis specification and morphogenesis in the mouse embryo require *Nap1*, a regulator of WAVE-mediated actin branching

Andrew S. Rakeman[1,2] and Kathryn V. Anderson[1,*]

Dynamic cell movements and rearrangements are essential for the generation of the mammalian body plan, although relatively little is known about the genes that coordinate cell movement and cell fate. WAVE complexes are regulators of the actin cytoskeleton that couple extracellular signals to polarized cell movement. Here, we show that mouse embryos that lack Nap1, a regulatory component of the WAVE complex, arrest at midgestation and have defects in morphogenesis of all three embryonic germ layers. WAVE protein is not detectable in *Nap1* mutants, and other components of the WAVE complex fail to localize to the surface of *Nap1* mutant cells; thus loss of *Nap1* appears to inactivate the WAVE complex in vivo. *Nap1* mutants show specific morphogenetic defects: they fail to close the neural tube, fail to form a single heart tube (cardia bifida), and show delayed migration of endoderm and mesoderm. Other morphogenetic processes appear to proceed normally in the absence of Nap1/WAVE activity: the notochord, the layers of the heart, and the epithelial-to-mesenchymal transition (EMT) at gastrulation appear normal. A striking phenotype seen in approximately one quarter of *Nap1* mutants is the duplication of the anteroposterior body axis. The axis duplications arise because Nap1 is required for the normal polarization and migration of cells of the Anterior Visceral Endoderm (AVE), an early extraembryonic organizer tissue. Thus, the *Nap1* mutant phenotypes define the crucial roles of Nap1/WAVE-mediated actin regulation in tissue organization and establishment of the body plan of the mammalian embryo.

KEY WORDS: Morphogenesis, Cell migration, Axis specification, Nap1, WAVE, Mouse embryo

INTRODUCTION

Cell-type specification in the mammalian embryo depends on the interplay between intercellular signaling events that determine cell fate and morphogenetic movements that regulate the positions of the signal-producing cells and their target tissues. Despite the essential role of cell movements in the establishment of the body plan, the molecular genetic analysis of mouse development has focused on the signaling pathways and transcription factors that control cell fate, and we understand much less about the genetic control of embryonic cell migration and tissue morphogenesis.

Gastrulation in the mouse, which establishes the three definitive germ layers from the single-cell layer of the epiblast, consists of a sequence of interdependent morphogenetic movements. Gastrulation initiates at E6.5 with the formation the primitive streak at one position on the circumference of the proximal epiblast; the position of the primitive streak defines the future posterior of the embryo. At the primitive streak, cells of the epiblast undergo an epithelial-to-mesenchymal transition (EMT), exit the primitive streak, enter either the mesodermal or endodermal germ layers, and then migrate anteriorly to form the definitive endoderm and mesoderm germ layers (Tam and Behringer, 1997). The EMT depends on Fgf signaling, which leads to the transcriptional downregulation of E-cadherin as cells traverse the primitive streak, which allows them to migrate away from the primitive streak in the mesodermal and endodermal layers (Ciruna and Rossant, 2001). The position and time that mesoderm cells move through the primitive streak is crucial for their fate: extraembryonic and cardiac mesoderm exit the primitive streak first, followed by paraxial mesoderm, which is generated by the middle primitive streak, and the node and notochord, which arise from the anterior primitive streak (Tam and Behringer, 1997).

It has been proposed that the position of the primitive streak in the posterior epiblast depends on the earlier movement of a group of extraembryonic cells, the anterior visceral endoderm (AVE). At the onset of gastrulation, the AVE overlies the anterior epiblast at the boundary between embryonic and extraembryonic regions. The AVE cells secrete Cerl, Lefty1 and Dkk1, which inhibit the Nodal and Wnt pathways that are required for primitive streak formation; this restricts the position of the primitive streak to a single site opposite the AVE (Lu et al., 2001). The cells that will become the AVE originate in the visceral endoderm at the distal tip of the egg cylinder at E5.0 when they begin to express characteristic molecular markers, including the transcription factors Hex and Hesx1. Between E5.5 and E6.0 the AVE cells migrate from their initial distal position to the proximal limit of the epiblast (Thomas et al., 1998).

Time-lapse imaging of Hex-GFP-expressing AVE cells has demonstrated that AVE cells migrate actively through the visceral endoderm: they become polarized and extend filopodia in the direction of migration and appear to move in response to a directional cue (Srinivas et al., 2004). Embryological ablation and transplantation experiments suggest that extraembryonic ectoderm may be the source of chemotactic signals that direct AVE migration (Rodriguez et al., 2005). In addition, inhibition of Nodal or Wnt signaling can reorient the direction of AVE migration (Kimura-Yoshida et al., 2005; Yamamoto et al., 2004), and the Nodal inhibitor *Lefty1* and *Wnt3* are asymmetrically expressed in the visceral endoderm at the time of AVE migration (Rivera-Pérez and

[1]Developmental Biology Program, Sloan-Kettering Institute, 1275 York Avenue, New York, NY 10021, USA. [2]Biochemistry, Cell and Molecular Biology Program, Weill Graduate School of Medical Sciences, Cornell University, 445 East 69th Street, New York, NY 10021, USA.

*Author for correspondence (e-mail: k-anderson@sloankettering.edu)

Accepted 5 June 2006

Magnuson, 2005; Takaoka et al., 2006). However, the molecular mechanisms and signals that provide the force and directionality of AVE migration in the normal embryo are not clear.

Cell migration depends on reorganization of the actin cytoskeleton that is mediated, in part, by proteins of the related WASP and WAVE families. WASP is auto-regulated by an inhibitory domain that prevents interaction with the ARP2/3 actin-nucleating complex. Binding of CDC42 to WASP relieves WASP auto-inhibition, allowing WASP to bind and activate ARP2/3, and promote formation of filopodia at the leading edge of migrating cells. WAVE proteins lack an auto-inhibitory domain and purified WAVE activates ARP2/3 constitutively (Bompard and Caron, 2004). WAVE is regulated by a complex of the Sra1, Nap1, Abi1 and HSPC300 proteins, which mediates responses to Rac (which binds Sra1), as well as to Nck (which binds Nap1) and Abl (which binds Abi1) (Echarri et al., 2004; Eden et al., 2002; Gautreau et al., 2004; Innocenti et al., 2004; Kobayashi et al., 1998; Steffen et al., 2004). Because the activities of Nck, Rac and Abl are regulated by intercellular signals, the components of the WAVE complex couple extracellular cues to the formation of lamellipodia at the leading edge of migrating cells.

The WAVE complex is crucial for diverse aspects of morphogenesis during development, including chemotactic movement of *Dictyostelium* amoebae (Blagg et al., 2003; Ibarra et al., 2006), axon pathfinding in *Drosophila* (Hummel et al., 2000) and spreading of the surface ectoderm in *C. elegans* (Soto et al., 2002). However, the roles of the WAVE complex in the morphogenetic events required for early vertebrate development have not been studied. Two murine *WAVE* genes, *WAVE1* and *WAVE2*, are expressed in the early embryo and appear to have overlapping functions in early development, as both single mutants survive beyond midgestation without gross morphological defects (Soderling et al., 2003; Yamazaki et al., 2003; Yan et al., 2003). *Abi2* mutants are viable and do not have morphological defects (Grove et al., 2004), whereas mutants in *Abi1*, either of the two *Sra* genes and *Hspc300* have not been described.

Here, we demonstrate that *Nap1*, the only member of its gene family expressed in the early mouse embryo, is essential for specific aspects of early morphogenesis. We confirm that Nap1 is required for the stability of WAVE and the membrane localization of WAVE complex proteins in embryonic cells. Based on the phenotypes of mutant embryos, we find that Nap1 and WAVE play specific roles in the regulation of migration of the mesoderm and endoderm, and in neural tube closure. In addition, we find that Nap1 regulates anteroposterior axis formation because it is required for normal polarization and migration of cells in the AVE. Our findings demonstrate that proper AVE migration is required for localized expression of the signals that determine the position of the primitive streak.

MATERIALS AND METHODS

Mouse strains and genotyping

We identified *Nap1^{khlo}* in a screen for recessive ethylnitrosourea-induced mutations (García-García et al., 2005). *Nap1^{khlo}* mutant mice were genotyped based on linkage to flanking SSLP markers (D2MIT94 and D2SKI328; http://mouse.ski.mskcc.org/). Phenotypic analysis was carried out in congenic C3HeB/FeJ animals. Two ES cell lines (XE068 and XE133) carrying gene trap insertions in the *Nap1* gene were obtained from BayGenomics. Both lines contained identical insertions 504 base pairs downstream of exon 24 of *Nap1*. Mice derived from both ES cell clones produced identical phenotypes and are collectively referred to as *Nap1^{GT}*. *Nap1^{GT}* mice were genotyped by PCR using primers to detect the *neo* gene (Jackson Laboratories; IMR013, IMR014, IMR015 and IMR016) or using primers that specifically amplified the wild-type (P1, 5′-CCAGATGG-CTGCACTCTTTA-3′; P2, 5′-CGTTCCTGAGAGGACAGAGC-3′) or *Nap1^{GT}* (P1, P3, 5′-TCTAGGACAAGAGGGCGAGA-3′) allele. The *Hex-GFP* transgene was detected by PCR using primers specific to *GFP* (Jackson Laboratories; IMR872, IMR1416).

Genetic mapping of *khlo*

The *khlo* mutation was mapped between *D2SKI308* and *D2SKI324* (http://mouse.ski.mskcc.org) in a backcross panel of 911 opportunities for recombination between C57BL/6J and C3HeB/FeJ or CAST/EiJ. Candidate genes in the critical interval were identified based on physical map information from Ensembl and the Celera Discovery System, and sequenced from RT-PCR products amplified from E8.5 *Nap1^{khlo}* and wild-type C57BL/6J RNA samples. The *Nap1* transcript amplified from four out of four *Nap1^{khlo}* mutant embryos contained a T to C transition mutation at nucleotide 50 of the *Nap1*-coding region.

Analysis of *khlo* mutant embryos

In situ hybridization, immunofluorescence and X-gal staining were carried out as described (Eggenschwiler and Anderson, 2000). Embryos for histological analysis were fixed in 4% paraformaldehyde in the decidual tissue, embedded in paraffin and sections were taken every 8 μm. Sections were stained with Hematoxylin and Eosin according to standard protocols.

Western blotting

Embryos were lysed in RIPA buffer with a protease inhibitor cocktail (Roche). Total protein concentration was estimated by Bradford assay and approximately 20 μg of total embryo extract was subject to western blotting. Bands were detected with ECL Plus (Amersham), and band intensities were measured from digital scans of films using ImageJ software (NIH).

Explant analysis

Primary explant cultures of nascent mesoderm, epiblast and primitive streak were generated as described (Burdsal et al., 1993; Ciruna and Rossant, 2001). The explants were cultured for 24-48 hours on fibronectin (BD Biosciences). Mesoderm migration in primitive streak explants was measured on digital photomicrographs using ImageJ software (NIH).

Analysis of Hex-GFP expression

Embryos from *Nap1^{khlo}*/+; *Hex-GFP*/+ intercrosses were dissected at E6.0 and fixed in 4% paraformaldehyde for one hour on ice. GFP-positive embryos were counterstained with rhodamine-phalloidin (Molecular Probes) and scanned on an inverted Leica TCS SP2 confocal microscope. Image stacks were assembled and analyzed using Volocity software (Improvision).

Antibodies and reagents

Polyclonal anti-Nap1 antiserum was raised against a C-terminal peptide (CHAVYKQSVTSSA), as described (Eden et al., 2002; Kitamura et al., 1996; Steffen et al., 2004). Anti-Abi1 monoclonal antibody was a generous gift from G. Scita (Milan). Polyclonal antiserum against Sra1 was a generous gift from T. Stradal (Braunschweig). Commercial antibodies used were: anti-E-cadherin (Sigma), anti-cortactin (Upstate), anti-WAVE1 (BD Transduction Laboratories) and anti-γ-tubulin (Sigma). Fluorescent secondary antibodies were from Jackson Laboratories and Molecular Probes. HRP-conjugated secondary antibodies were from Zymed and Amersham. Filamentous actin was detected with rhodamine-conjugated phalloidin (Molecular Probes) and nuclei were visualized with DAPI (Sigma).

RESULTS

Loss of *Nap1* causes morphogenetic defects and midgestation lethality

We identified two recessive mutations in the mouse *Nap1* gene (also known as *Nap125*, *Nckap1* or *Hem2*) that caused striking morphological defects and lethality at E9.0. The first allele, *khlo*, was identified in an ENU mutagenesis screen based on a set of prominent morphogenetic defects in the midgestation (E9.0) mouse embryo (García-García et al., 2005). Mutants arrested development

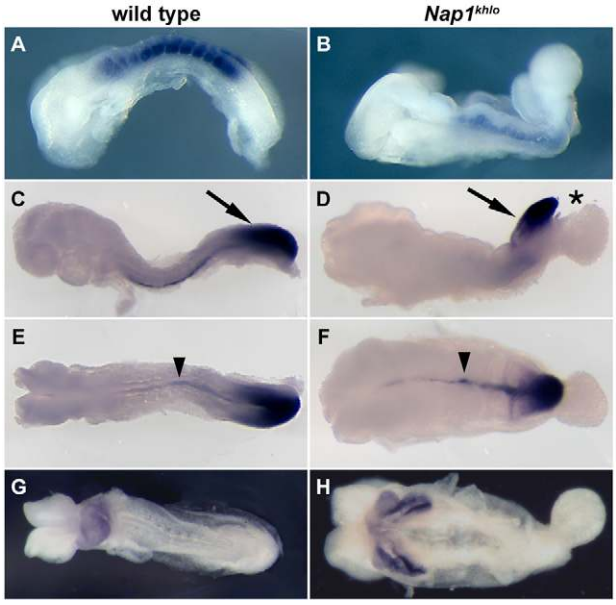

Fig. 1. Morphogenetic defects in *Nap1^{khlo}* mutant embryos. (**A**,**B**) *Mox1* expression marks the somites and presomitic mesoderm of wild-type E8.5 embryos (A) and reveals the small somites of E8.5 *Nap1^{khlo}* embryos (B). (**C-F**) Brachyury (*T*) expression marks the primitive streak and notochord in E8.5 wild-type (C,E) and *Nap1^{khlo}* (D,F) embryos. In the mutant, the primitive streak (arrow) was distended and the allantois failed to fuse with the chorion (asterisk). The notochord (arrowhead) appeared normal in *Nap1^{khlo}* mutants. (**G**,**H**) The pan-cardiac marker *Nkx2.5* was expressed in a single heart in wild-type embryos (G) and in the two lateral heart domains in *Nap1^{khlo}* mutant embryos (H). Anterior is to the left in all panels.

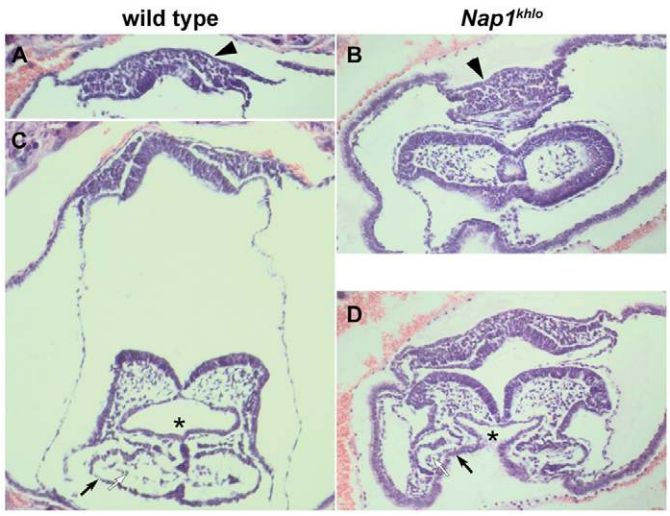

Fig. 2. Histological analysis of E8.5 *Nap1^{khlo}* mutants. (**A**,**B**) The primitive streak region of wild-type embryos contained a small number of mesenchymal cells (A, arrowhead), whereas the *Nap1^{khlo}* primitive streak contained a mass of disorganized mesenchymal cells (B, arrowhead). (**C**,**D**) The layered organization of myocardium (black arrows) and endocardium (white arrows) in the wild-type heart (C) was present in *Nap1^{khlo}* mutant hearts (D). The foregut (asterisk) formed a closed pocket in wild-type embryos (C), but failed to close in *Nap1^{khlo}* mutants (D).

prior to embryonic turning, with only 5-6 pairs of small somites when wild-type littermates had 8-12 pairs of somites (Fig. 1A,B). At E8.5, *khlo* embryos accumulated a mass of disorganized mesenchymal cells at the primitive streak, the source of new mesoderm and endoderm (Fig. 1D, Fig. 2B). This phenotype is seen in embryos with defects in migration of mesoderm away from the primitive streak (Bladt et al., 2003; Meyers et al., 1998; Xue et al., 2001), suggesting that the *khlo* mutation affected cell migration. The two *khlo* heart primordia failed to fuse to form a single heart tube (cardia bifida; Fig. 1H, Fig. 2D), and the underlying endoderm failed to close to form the foregut pocket (Fig. 2D). Closure of neural ectoderm into a tube failed completely in *khlo* embryos (Fig. 1B; data not shown). Because most mesodermal and neural cell types were specified normally in *khlo* embryos (Fig. 1B,D,F,H; see also Fig. S1 in the supplementary material), it appeared that the mutant phenotypes were the result of defects in cell and tissue movements. In addition to these morphogenetic defects, a fraction of *khlo* embryos showed duplications of the anteroposterior body axis of varying severity (Fig. 3B,C,E; see below).

We mapped the *khlo* mutation to a 1.4 Mb region on chromosome 2 that contained nine transcription units including the *Nap1* gene (Fig. 4A). The mutant allele was associated with a missense mutation in an evolutionarily conserved residue (L17P) near the N terminus of the *Nap1* open reading frame (Fig. 4B). We generated a second allele of the gene from an ES cell line that carried a gene-trap insertion (Stryke et al., 2003) into *Nap1* (*Nap1^{GT}*) that should encode a truncated protein fused to β-geo (Fig. 4C,D). Embryos homozygous for the gene trap allele, as well as *khlo*/*Nap1^{GT}* embryos, arrested at E9.0 with phenotypes similar to that of *khlo* (Fig. 4F; data not shown). The similar embryonic phenotypes caused by the two alleles and their failure to complement confirmed that the early lethality and morphological abnormalities of the mutants were the result of the loss of *Nap1* activity. The phenotypes of *Nap1^{GT}* homozygous and *Nap1^{GT}*/*Nap1^{khlo}* embryos were slightly weaker than that of *Nap1^{khlo}* homozygotes (see below), which suggested that *Nap1^{GT}* retained some wild-type activity. Consistent with this hypothesis, we detected a small amount of normally spliced *Nap1* transcript in RNA samples from *Nap1^{GT}* homozygous embryos by RT-PCR (data not shown).

The Nap1 protein was expressed in all three germ layers of the embryo as well as in the visceral endoderm during gastrulation (Fig. 5A,B). Nap1 was also expressed in all cell types at midgestation (Fig. 5C-E; data not shown). The protein was enriched in both apical and basal regions of epithelia (Fig. 5A-E).

Nap1 is essential for stability and membrane localization of the WAVE complex in embryonic cells

Previous RNA interference studies in cultured cells indicated that both Nap1 and its blood cell-specific homolog Hem1 are required for the stability of WAVE proteins (Steffen et al., 2004; Weiner et al., 2006). Although we did not detect WAVE2 protein in early wild-type embryos (data not shown), three isoforms of WAVE1 were observed in extracts from E8.5 wild-type embryos. WAVE1 levels were reduced more than 10-fold in *Nap1^{khlo}* mutant embryo extracts (0.06±0.03, n=5), and by approximately twofold in *Nap1^{khlo}* heterozygous embryo extracts (0.44±0.09, n=5, Fig. 6A); thus, Nap1 is required for WAVE stability in the early embryo.

The WAVE complex localizes to lamellipodia, and this membrane localization is essential for its activity (Innocenti et al., 2004; Steffen et al., 2004). RNA interference experiments have indicated that

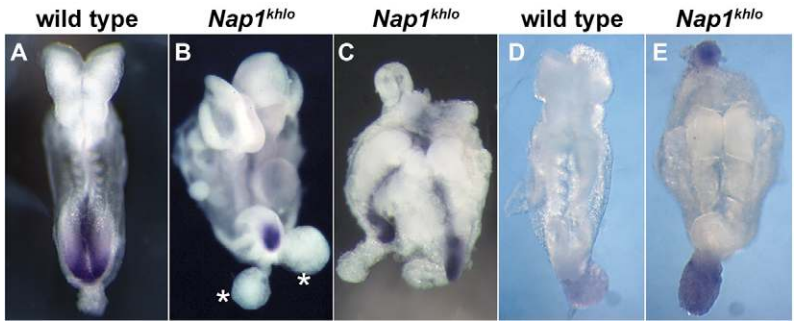

Fig. 3. Axis duplications in *Nap1*^{khlo} mutants. (**A-C**) *T* expression. (A) Wild-type embryos have a single allantois, and a brachyury-expressing primitive streak and notochord at E8.5. Approximately one quarter of *Nap1*^{khlo} homozygotes showed a partial or complete duplication of the anteroposterior axis. In some mutants, the allantois was duplicated (B, asterisk), whereas nearly the entire body axis, including the primitive streak and notochord, was duplicated in the most severely affected *Nap1*^{khlo} mutants (C). (**D**,**E**) *Tbx4* expression marks the allantois in a wild-type embryo (D) and in a *Nap1*^{khlo} mutant with an ectopic allantois (E). Anterior is up in all panels.

Nap1 is required for membrane localization of the WAVE complex components Sra1 and Abi1 (Steffen et al., 2004). In primary cultures of wild-type E7.5 mesodermal cells, Sra1 and Abi1 localized to the leading edge of migrating cells (Fig. 6B,D). By contrast, Sra1 and Abi1 could not be detected on the surface of *Nap1*^{khlo} mutant mesodermal cells (Fig. 6C,E). We observed a low level of Sra1 and Abi1 surface localization in *Nap1*^{GT} cells (data not shown), consistent with the slightly milder phenotype of *Nap1*^{GT} embryos.

The destabilization of WAVE and the mislocalization of Abi and Sra1 in *Nap1*^{khlo} cells confirm the conclusions from RNA interference experiments that Nap1 is required for WAVE stability and WAVE complex membrane localization in vivo. These phenotypes demonstrate that the *Nap1*^{khlo} mutation is a strong loss-of-function or null allele, and that no other gene can compensate for loss of *Nap1* in the embryo.

Nap1 mutant mesodermal cells lack normal lamellipodia and fail to polarize

Because WAVE proteins regulate the reorganization of the actin cytoskeleton required for cell migration, we assessed the organization of the actin cytoskeleton in cells isolated from *Nap1*^{khlo} embryonic tissue layers. The epiblast (the epithelial layer of the early embryo) and mesoderm layers were isolated from E7.5 embryos, cultured in conditions where they retain their epithelial and mesenchymal character (Burdsal et al., 1993), and stained with phalloidin to visualize the actin cytoskeleton. The actin cytoskeleton of *Nap1*^{khlo} mutant epiblast cells was indistinguishable from that of wild-type cells (Fig. 6F,G). By contrast, phalloidin staining showed that mesoderm cells from *Nap1*^{khlo} embryos were more compact than wild-type mesoderm cells, and had a collapsed network of stress fibers surrounding the nucleus (Fig. 6H,I). Wild-type

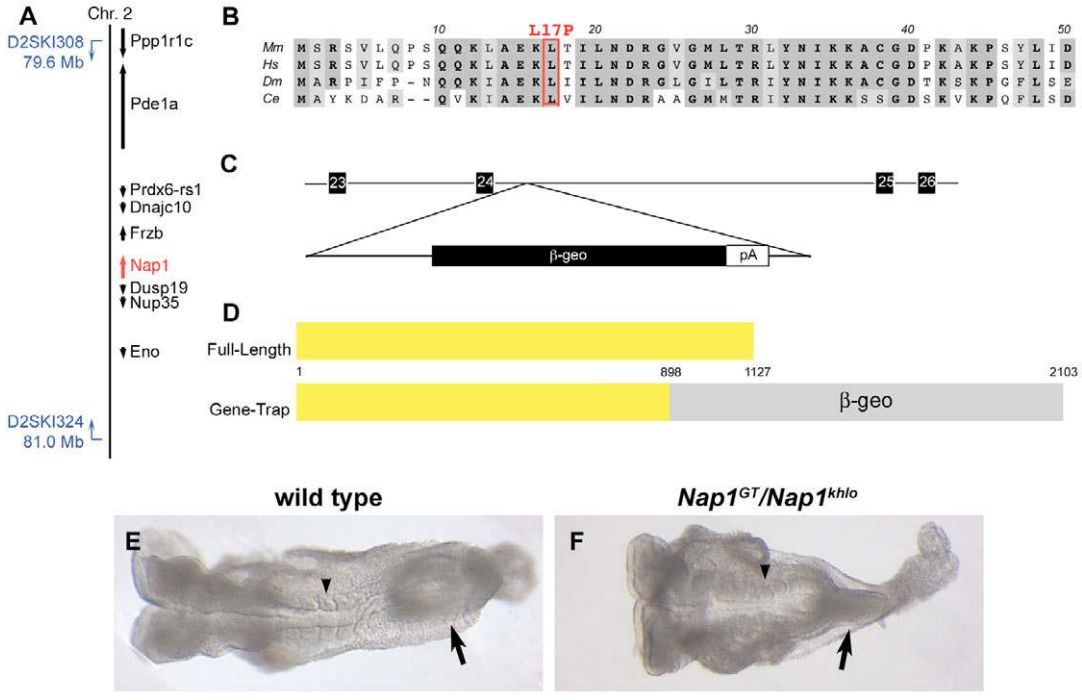

Fig. 4. Mapping and molecular characterization of *Nap1* alleles. (**A**) The *khlo* mutation mapped between the SSLP markers D2SKI308 and D2SKI324 on chromosome 2 (http://mouse.ski.mskcc.org/). (**B**) Alignment of the N-terminal region of murine Nap1 (*Mm*) and its human (*Hs*), *Drosophila melanogaster* (*Dm, kette*) and *C. elegans* (*Ce, gex-3*) homologs. The leucine residue mutated in *Nap1*^{khlo} is conserved in all four species (red box) and occurs in a leucine-rich region of the protein. (**C**,**D**) The *Nap1*^{GT} insertion trapped the *Nap1* transcript after exon 24 (C), creating a fusion of the 898 N-terminal amino acids of Nap1 with β-geo (D). (**E**,**F**) *Nap1*^{khlo}/*Nap1*^{GT} mutants (F) arrested at E8.5 with multiple morphogenetic defects, including a distended primitive streak (arrows) and malformed somites (arrowheads); compare with wild type (E). Anterior is to the left in E and F.

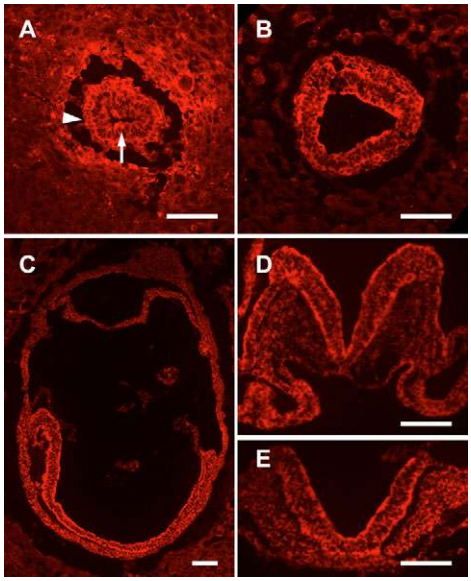

Fig. 5. Expression of Nap1 during development. (**A**) Nap1 protein was present in the epiblast (arrow) and visceral endoderm (arrowhead) in transverse sections of E6.5 embryos. (**B**) Nap1 is present in all three germ layers in transverse sections of E7.5 embryos, and is enriched in the apical region of the epiblast. (**C-E**) Nap1 was present in all embryonic structures in sagittal sections of E8.0 embryos (C) and was expressed in all tissues in transverse sections of E8.5 embryos (D,E). At E8.5, Nap1 was enriched in both apical and basal regions of the cells in the neural tube (D,E); based on the Nap1 mutant phenotypes, it is likely that this localization of Nap1 is required for neural tube closure. Anterior is to the left in A-C and dorsal is up in D and E. Scale bars: 100 μm.

mesodermal cells were polarized and had large lamellipodia, as visualized by staining for cortactin, an actin-binding protein that is enriched in lamellipodia (Weed et al., 2000) (Fig. 6J). By contrast, *Nap1*^{khlo} mesodermal cells were surrounded by many short protrusions, had only small lamellipodia, and lacked clear polarity (Fig. 6K). Thus, mesodermal cells isolated from *Nap1*^{khlo} mutants lacked the actin organization required for efficient polarized cell migration, similar to the cellular phenotypes seen in cultured *WAVE2* mutant fibroblasts (Yan et al., 2003), or in cell lines depleted for Nap1, Hem1, Sra1 or Abi1 activity by small interfering RNAs (Innocenti et al., 2004; Steffen et al., 2004; Weiner et al., 2006).

Defects in mesoderm and endoderm migration in *Nap1*^{khlo} embryos

In the gastrulating embryo, the mesoderm and endoderm migrate through the primitive streak and then spread away to create the definitive germ layers of the embryo. To assess the ability of the mutant mesoderm cells to migrate, we analyzed primitive streak explants from E7.5 embryos; these explants include both the epiblast and nascent mesoderm, and continue to generate migrating mesodermal cells in culture (Ciruna and Rossant, 2001). Wild-type primitive streak explants produced E-cadherin-negative mesenchymal cells that migrated away from the epiblast and traveled approximately 350 μm over 24 hours (Fig. 7A). By contrast, mesenchymal cells produced by *Nap1*^{khlo} mutant primitive streaks downregulated E-cadherin, but failed to migrate and accumulated beneath the epiblast (Fig. 7B). Thus, Nap1 was absolutely required for mesoderm migration in culture.

In contrast to its complete failure in culture, mesoderm migration was only partially disrupted in the intact embryo. Nascent mesodermal cells of *Nap1*^{khlo} embryos did not migrate as efficiently as wild-type cells: as early as E7.5, mesoderm accumulated adjacent to the *Nap1*^{khlo} primitive streak, forming a layer that was three to four cells thick, whereas wild-type embryos had only a single layer of mesodermal cells between the primitive streak and the endoderm (Fig. 7C,D). Despite this defect, the majority of mesoderm cells spread around the circumference of E7.5 mutant embryos (Fig. 7D), and *Cripto* and *Lim1*, markers of the nascent mesoderm, were expressed in their normal domains around the embryonic circumference in the mutants (Fig. 8A-D). Furthermore, lateral plate, cardiac and axial mesoderm were properly specified and had moved to their normal positions at E8.0-E8.5 (Fig. 1F,H; data not shown). Only migration of the paraxial mesoderm (the precursor of the somitic mesoderm), the last mesodermal cell type to transit the primitive streak, was clearly disrupted in *Nap1*^{khlo} mutants. Only a few small somites formed, although *Mox1* expression revealed that some paraxial mesoderm cells did successfully migrate away from the primitive streak (Fig. 1B). Thus, in contrast to the dramatic defect in primitive streak explants, mesoderm migration in the embryo was only modestly disrupted; this discrepancy suggests that mesoderm migration in vivo depends on both Nap1-dependent and Nap1-independent mechanisms that are not mimicked in culture.

Although cardiac mesoderm cells were present in the two lateral cardiac anlagen of *Nap1*^{khlo} embryos, these primordia failed to move ventrally to fuse in a single heart tube, which resulted in cardia bifida (Fig. 1H). Despite the abnormal position of *Nap1*^{khlo} hearts, the

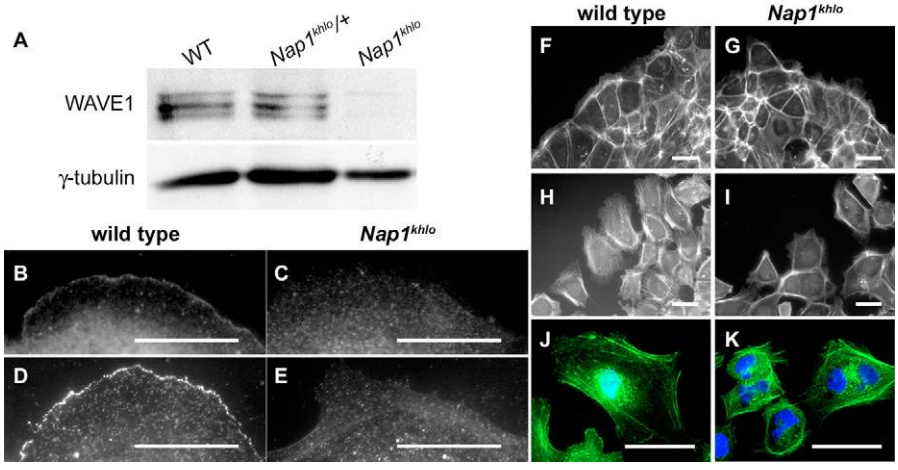

Fig. 6. Behavior of WAVE complex components in *Nap1*^{khlo} mutants. (**A**) Western blot analysis of WAVE1 protein in E8.5 embryos, normalized to γ-tubulin levels. (**B-E**) Immunofluorescent staining shows that Sra1 (B,C) and Abi1 (D,E) are localized to the surface of wild-type (B,D) but not *Nap1*^{khlo} (C,E) primary mesodermal cells. Scale bars in B-E: 25 μm. (**F-I**) Actin structures in wild-type (F,H) and *Nap1*^{khlo} (G,I) epithelial (F,G) and mesodermal (H,I) cells, visualized by phalloidin staining. (**J**,**K**) Localization of the actin-binding protein cortactin (green) and DAPI (blue) in wild-type (J) and *Nap1*^{khlo} (K) mutant mesodermal cells. Scale bars in F-K: 50 μm.

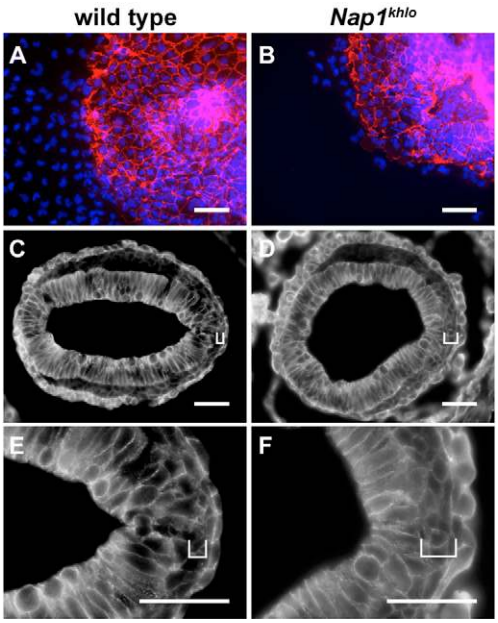

Fig. 7. Cell migration defects in *Nap1*^{khlo} explants and embryos. (**A**,**B**) Wild-type (A) and *Nap1*^{khlo} (B) primitive streak explants stained with DAPI (blue) and antibodies against E-cadherin (red) to distinguish the E-cadherin-expressing epithelial cells from E-cadherin-negative mesodermal cells. (**C-F**) Transverse sections of wild-type (C,E) and *Nap1*^{khlo} (D,F) E7.5 embryos stained for expression of E-cadherin. Brackets mark the layer of mesenchymal cells adjacent to the primitive streak; whereas a single layer of mesoderm cells lie adjacent to the primitive streak in wild type, 3-4 layers of mesoderm cells underlie the *Nap1*^{khlo} primitive streak. Scale bars: 100 μm.

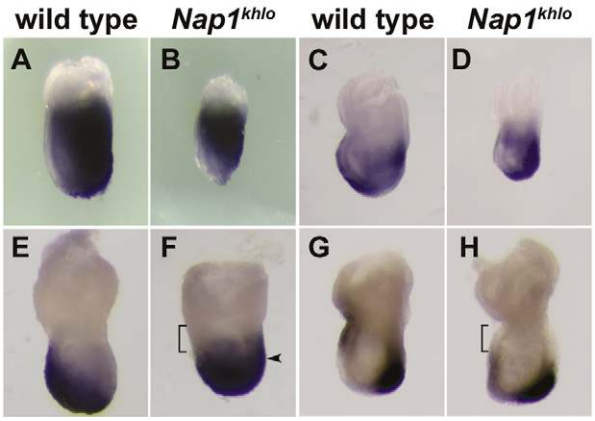

Fig. 8. Behavior of nascent mesoderm and endoderm. (**A-D**) *Cripto* (A,B) and *Lim1* (C,D) expression in nascent mesoderm cells; these markers occupied their normal domains in *Nap1*^{khlo} mutants (B,D) compared to wild-type embryos (A,C) at E7.5. (**E**,**F**) By E7.5, *Cerl*-expressing cells of the foregut migrated to the anterior of wild-type embryos (E), but failed to reach the anterior of *Nap1*^{khlo} mutant embryos (bracket, F), and instead accumulated adjacent to the primitive streak (arrowhead). (**G**,**H**) *Foxa2* expression in wild-type (G) and *Nap1*^{khlo} mutant embryos (H) at E7.5. The *Foxa2*-expressing foregut domain failed to reach the anterior of *Nap1*^{khlo} embryos (bracket). Anterior is to the left in all panels.

myocardial and endocardial tissue layers were organized normally (Fig. 2D) and the hearts could beat. Thus, the tissue reorganization required to generate the layered organization of the heart does not depend on Nap1, whereas the movement of the heart primordia to the midline does require Nap1.

The foregut endoderm underlying the heart failed to fuse to form the anterior gut tube in *Nap1*^{khlo} mutants (Fig. 2D), which suggested defective migration of the endoderm. We found that definitive endoderm cells, marked by expression of *Cerl*, exited the primitive streak of *Nap1*^{khlo} embryos, but they did not spread anteriorly. By E7.5, *Cerl*-expressing cells had arrived at the anterior of wild-type embryos, but accumulated adjacent to the primitive streak of mutant embryos (Fig. 8F,G). Similarly, *FoxA2*, a marker of the foregut, was expressed in fewer cells in mutants than in wild-type embryos and the mutant cells failed to reach the anterior (Fig. 8H,I). Delayed migration of the definitive endoderm is sufficient to account for failure of foregut closure (Constam and Robertson, 2000), and closure of the foregut is required for fusion of the lateral heart primordia (Constam and Robertson, 2000; Roebroek et al., 1998). Thus, the cardia bifida seen in *Nap1*^{khlo} mutant embryos may be secondary to delayed endoderm migration.

Axis duplications in *Nap1* mutant embryos

Although most of the phenotypes of *Nap1* mutant embryos could be attributed to defects in morphogenesis, approximately one quarter of *Nap1* mutants had a striking defect in patterning of the body axis. Primitive streak-derived structures were duplicated in 16% of E8.5 embryos homozygous for *Nap1*^{khlo} (13 out of 82) and 8% of *Nap1*^{GT} homozygotes (7 out of 86). In half of these embryos (6 out of 13 for *Nap1*^{khlo} and 4 out of 7 for *Nap1*^{GT}), only the allantois, the most posterior embryonic structure, was duplicated (Fig. 3B). In the other half, all primitive streak-derived structures, including the node and the notochord, were duplicated (Fig. 3C). In addition to these embryos, some *Nap1*^{khlo} homozygotes (3 out of 45) had a second allantois located anterior to the head (Fig. 3E).

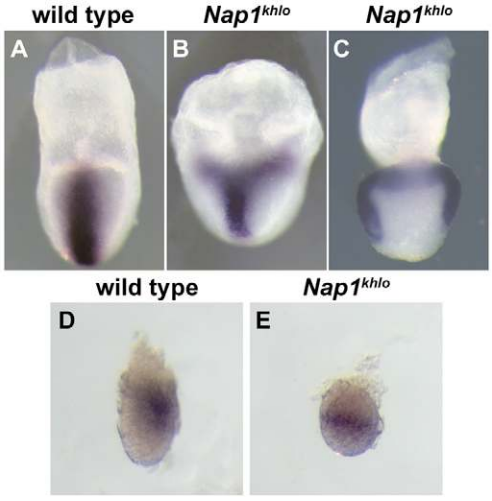

Fig. 9. Expanded domain of expression of primitive streak markers in *Nap1*^{khlo} mutants. (**A-C**) Posterior views of *T* expression in E7.5 wild-type (A) and *Nap1*^{khlo} embryos (B,C). These *Nap1*^{khlo} mutants expressed *T* ectopically at the embryonic-extraembryonic boundary (B) or in two distinct primitive streaks (C). (**D**,**E**) *Wnt3* is expressed in the posterior of E6.5 wild-type embryos (D), but is expressed around the circumference of *Nap1*^{khlo} mutants (E) at E6.5. Anterior is to the left in D and E.

Axis duplication can occur either because of duplication of the node (Merrill et al., 2004) or because of abnormal specification of the primitive streak (Pöpperl et al., 1997; Shawlot and Behringer, 1995). When assayed prior to formation of the node, approximately 20% (3 out of 16) of E7.5 *Nap1*^{khlo} embryos expressed the primitive streak marker brachyury (*T*) ectopically in two stripes or in a ring at the proximal end of the epiblast (Fig. 9A-C). Formation of the primitive streak requires Wnt3, and *Wnt3* expression in the posterior epiblast and adjacent visceral endoderm is the earliest known marker for the posterior pole of the embryonic axis (Rivera-Pérez and Magnuson, 2005). At E6.5, *Wnt3* expression was restricted to the posterior epiblast of wild-type embryos, but was expanded around the embryonic circumference in ~40% (3 out of 7) *Nap1*^{khlo} mutants (Fig. 9D,E). These results indicate that the axis duplications in *Nap1*^{khlo} embryos were caused by the failure to restrict primitive streak formation to a single site.

Axis duplication in *Nap1*^{khlo} mutants is caused by defective AVE migration

Specification of primitive streak position correlates with the migration of the AVE from its initial distal position to the future anterior side of the embryo before the onset of gastrulation (Beddington and Robertson, 1999). Because Nap1 is required for cell migration and for the restriction of the primitive streak to the posterior, we tested whether Nap1 was required for migration of the AVE. *Cerl* and *Hex* are expressed in overlapping but distinct populations of AVE cells (Yamamoto et al., 2004). The AVE, marked by either *Cerl* or *Hex*, failed to reach its normal proximal position at the embryonic/extraembryonic boundary in ~50% (6 out of 11) of the *Nap1*^{khlo} embryos examined at E6.5 and E7.5 (Fig. 10A-D). Using a *Hex-GFP* transgene (Srinivas et al., 2004), we were able to follow the behavior of individual AVE cells. By E6.0, all of the GFP-expressing cells had left the distal tip of the wild-type embryos (Fig. 10E,G), but in half (4 out of 8) of the *Nap1*^{khlo} embryos the majority of the Hex-GFP-expressing cells failed to migrate away from the distal pole (Fig. 10E,F), although some Hex-GFP-expressing cells reached the presumptive anterior (Fig. 10F). Additionally, in one embryo in which the majority of the GFP-expressing cells migrated to the presumptive anterior side of the embryo, a few GFP-positive cells were present on the posterior side of the embryo (Fig. 10H). We therefore conclude that Nap1 is required for efficient directional migration of the AVE and that inefficient migration of the AVE is the cause of the axis duplications seen in *Nap1* mutant embryos.

Cells of the wild-type AVE extend polarized processes during migration (Srinivas et al., 2004), and we had seen that *Nap1* was required for cellular polarity in explanted mesodermal cells. We therefore hypothesized that the defective AVE movement in *Nap1*^{khlo} mutants could be due to a defect in polarization of the AVE cells. Using the *Hex-GFP* transgene (Srinivas et al., 2004) to mark the AVE, we confirmed that AVE cells in wild-type E6.0 embryos were elongated and polarized in the direction of migration (Fig. 10I). By contrast, Hex-GFP-expressing cells in all *Nap1*^{khlo} mutant embryos examined (n=8), regardless of their position along the proximodistal axis, were more round and had no obvious leading-trailing polarity (Fig. 10J), a phenotype similar to that seen in explanted mesodermal cells (Fig. 6I,K). These data demonstrate that *Nap1* is required for the polarization of AVE cells and that this polarity is required for efficient migration of the AVE.

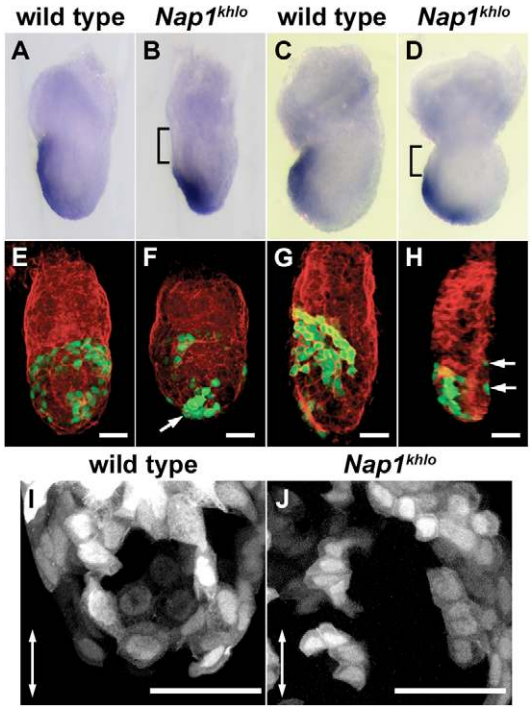

Fig. 10. AVE defects in *Nap1*^{khlo} mutants. (**A-D**) Cells of the AVE, marked by expression of *Cerl* at E6.5 (A,B) and *Hex* at E7.5 (C,D), were present at the embryonic-extraembryonic boundary of wild-type embryos (A,C), but failed to migrate completely in half of the *Nap1*^{khlo} mutants examined (B,D, brackets). Anterior is to the left. (**E-H**) All Hex-GFP-expressing cells migrated towards the anterior of wild-type embryos at E6.0 (E,G), but some Hex-GFP cells remained distal (F, arrow) or migrated to the posterior (H, arrows) in half of the *Nap1*^{khlo} embryos examined (green, Hex-GFP; red, phalloidin). Anterior is out in E and F, and to the left in G and H. (**I**,**J**) High magnification anterior views of the Hex-GFP-expressing cells in E6.0 wild-type (I) and *Nap1*^{khlo} (J) embryos. Vertical arrows in I and J represent the orientation of the proximodistal axis. Note that that although the wild-type AVE cells are elongated along the proximodistal axis, the *Nap1*^{khlo} cells are not. Scale bars in E-J: 50 μm.

DISCUSSION

Specific morphogenetic movements in the mouse embryo depend on Nap1 and the WAVE complex

Although it is clear that the WAVE complex is essential for the migration of cells in culture, its roles during development of the mouse embryo have not been defined. We find that Nap1, a component of the WAVE regulatory complex, is the only member of its gene family required in the early embryo and that *Nap1*^{khlo} mutant embryos appear to lack all WAVE complex activity. Thus, the *Nap1*^{khlo} phenotype defines the role of the WAVE complex in the morphogenetic events that shape the early mouse embryo.

Although *Nap1* is essential for survival of the embryo, not all morphogenetic events are disrupted in *Nap1*^{khlo} embryos. For example, *Nap1*, and therefore the regulated activity of WAVE, are absolutely required for the cell shape changes that allow neural tube closure. By contrast, the morphogenetic events that shape the notochord, the layers of the heart and the EMT during gastrulation appear to be normal in *Nap1*^{khlo} embryos. Most cell migration events in *Nap1*^{khlo} mutants are disrupted, although to varying degrees. Migration of AVE cells, which move as individuals, was consistently disrupted, although some AVE cells arrive at the correct final destination. Migration of the definitive endoderm, which migrates as an epithelial sheet, is severely retarded. Migration of the mesoderm, which migrates as loosely connected groups of cells, was

moderately retarded in vivo. Among the mesodermal subtypes, only the paraxial mesoderm showed significant disruption: only a few, small somites were specified in mutant embryos. As the paraxial mesoderm is the last mesodermal type to move through the primitive streak (Tam et al., 2001), the defect in paraxial mesoderm may represent the cumulative effects of slightly delayed mesoderm migration throughout the course of gastrulation; alternatively, paraxial mesoderm may be uniquely dependent on Nap1-mediated signals for migration.

In none of these cases (migration of the AVE, endoderm and mesoderm) does loss of Nap1 completely block cell migration in vivo. This finding is similar to that seen with mutations in *Dictyostelium NapA*, *PirA* and *Scar*, which encode the homologs of Nap1, Sra1 and WAVE (Blagg et al., 2003; Ibarra et al., 2006). *NapA*, *PirA* and *Scar* mutant cells are motile and can move towards a chemoattractant, but they move more slowly and fail to orient efficiently towards the chemoattractant. Thus, as in *Dictyostelium*, embryonic cell migrations are regulated both by WAVE and by other components that collaborate with WAVE to promote directional migration.

Tissue-specific regulation of WAVE

The phenotypes of mouse mutants that lack *Nck*, *Abl* or *Rac*, the components that act upstream of the WAVE complex, suggest that different signals regulate the WAVE complex in the different cell types. Embryos that lack both *Nck1* and *Nck2* arrest at approximately E9.0 and have an external morphology similar to that of $Nap1^{khlo}$ mutants (Bladt et al., 2003). This phenotypic similarity suggests that receptor tyrosine kinase signaling, mediated by Nck, could be the central regulator of the WAVE complex during mesoderm and endoderm migration. The neural tube of *Nck1; Nck2* double mutants closes in the trunk, in contrast to the completely open neural tube of $Nap1^{khlo}$ embryos, which suggests that Nck does not regulate neural tube closure. However, embryos that lack two *Abl* genes, *Abl* and *Arg*, completely fail to close the neural tube (Koleske et al., 1998). Thus, the Abl kinases are good candidates to act upstream of WAVE in neural tube closure. *Rac1* is required for survival of the nascent mesoderm (Sugihara et al., 1998), precluding analysis of its role in germ layer migration or neural tube closure. Migration of the AVE has not been analyzed in *Rac1* mutants or in *Nck1; Nck2* or *Abl; Arg* double mutant embryos, so it is not clear which of these upstream regulators control the WAVE complex in the AVE.

Cell migration is required for specification of a single body axis and acts upstream of Wnt3

Because movement of the AVE correlates with primitive streak formation, it has been hypothesized that AVE movement determines primitive streak position and orientation of the anteroposterior axis. However, all the genes that have been previously shown to be required for AVE migration, such as *Cripto*, *Otx2* and *Lim1*, regulate the expression and/or activity of the Wnt and Nodal signals that control the primitive streak fate (Ding et al., 1998; Kinder et al., 2001; Perea-Gomez et al., 2001). As a result, the phenotypes of these mutants do not formally distinguish between the possibility that AVE migration is required to specify the position of the primitive streak and the possibility that the same signaling molecules act twice to control AVE migration and primitive streak formation (Ding et al., 1998; Perea-Gomez et al., 2001; Shawlot et al., 1998). Because Nap1 is dedicated to the regulation of the cytoskeleton, the coupled $Nap1^{khlo}$ phenotypes of disrupted AVE migration and axis duplication demonstrate that movement of the AVE is required for normal positioning of the primitive streak.

The nature of the earliest events that define the position of the anteroposterior axis is still controversial. Recent data have suggested that *Wnt3* expression in the posterior visceral endoderm may precede AVE migration (Rivera-Pérez and Magnuson, 2005) and that overexpression of Wnts can block AVE migration (Kimura-Yoshida et al., 2005). These observations suggested that the direction of AVE migration is a consequence of a pre-existing anteroposterior polarization of Wnt signaling. However, the AVE migrates normally in *Wnt3* mutant embryos (Liu et al., 1999). In addition, our data demonstrate that AVE movement is crucial for the restriction of *Wnt3* expression to the posterior of the embryo. We therefore argue that AVE migration begins before Wnt signaling is localized and that other, non-Wnt, signals initiate the polarized migration of the AVE cells. Our findings would, however, be consistent with the possibility that once AVE movement is initiated, localized Wnt signals reinforce the direction of AVE migration.

While AVE migration and the domain of *Wnt3* expression appear to be directly coupled, additional events must regulate the formation of the primitive streak and the definitive anteroposterior axis. Although we find that the degree of migration of the AVE is correlated to the domain of *Wnt3* expression, the frequency of axis duplication at E8.5 was significantly lower than the frequency of AVE migration defects (13 out of 82 versus 9 out of 18; χ^2, $P \leq 0.01$). We infer that the expanded *Wnt3* domain represents the region that is competent to form a primitive streak, but additional regulative events restrict primitive streak formation to a single site in all but the most severely affected mutants. Consistent with these observations, embryological experiments in the chick have demonstrated the existence of a streak-derived inhibitor that prevents ectopic streak formation (Bertocchini et al., 2004).

We propose that several mechanisms act in concert to insure formation of a single primitive streak and, therefore, a single anteroposterior body axis. The migration of AVE cells is regulated by Nap1 and also by Nap1-independent mechanisms. AVE migration controls the size of the domain competent to form a primitive streak, marked by *Wnt3* expression. If the AVE migrates slowly or does not reach the correct final position, a feedback loop is initiated from the primitive streak that prevents the specification of an ectopic primitive streak. Only when more than one mechanism fails, is it possible for two stable primitive streaks to form and direct the specification of more than one body axis.

We thank M. Wyler for initial mapping of *khlo*; M. Zhao for the Nap1 antibody; T. Rodriguez and T. Magnuson for providing the *Hex-GFP* transgenic mice; G. Scita and T. Stradal for providing antibodies; the Sloan Kettering Molecular Cytology Core Facility for assistance with confocal microscopy and image analysis; M. Baylies, T. Bestor, and members of the Anderson lab for comments on the manuscript; and L. M. Rakeman for naming *khlo*. $Nap1^{GT}$ ES cells were obtained from BayGenomics. Genome sequence analysis used Ensembl and the Celera Discovery System and associated databases. The work was supported by NIH grant HD35455 to K.V.A.

Supplementary material

Supplementary material for this article is available at http://dev.biologists.org/cgi/content/full/133/16/3075/DC1

References

Beddington, R. S. and Robertson, E. J. (1999). Axis development and early asymmetry in mammals. *Cell* **96**, 195-209.

Bertocchini, F., Skromne, I., Wolpert, L. and Stern, C. D. (2004). Determination of embryonic polarity in a regulative system: evidence for endogenous inhibitors acting sequentially during primitive streak formation in the chick embryo. *Development* **131**, 3381-3390.

Bladt, F., Aippersbach, E., Gelkop, S., Strasser, G. A., Nash, P., Tafuri, A., Gertler, F. B. and Pawson, T. (2003). The murine Nck SH2/SH3 adaptors are important for the development of mesoderm-derived embryonic structures and for regulating the cellular actin network. *Mol. Cell. Biol.* **23**, 4586-4597.

Blagg, S. L., Stewart, M., Sambles, C. and Insall, R. H. (2003). PIR121 regulates pseudopod dynamics and SCAR activity in *Dictyostelium*. *Curr. Biol.* **13**, 1480-1487.
Bompard, G. and Caron, E. (2004). Regulation of WASP/WAVE proteins: making a long story short. *J. Cell Biol.* **166**, 957-962.
Burdsal, C. A., Damsky, C. H. and Pedersen, R. A. (1993). The role of E-cadherin and integrins in mesoderm differentiation and migration at the mammalian primitive streak. *Development* **118**, 829-844.
Ciruna, B. and Rossant, J. (2001). FGF signaling regulates mesoderm cell fate specification and morphogenetic movement at the primitive streak. *Dev. Cell* **1**, 37-49.
Constam, D. B. and Robertson, E. J. (2000). Tissue-specific requirements for the proprotein convertase furin/SPC1 during embryonic turning and heart looping. *Development* **127**, 245-254.
Ding, J., Yang, L., Yan, Y. T., Chen, A., Desai, N., Wynshaw-Boris, A. and Shen, M. M. (1998). *Cripto* is required for correct orientation of the anterior-posterior axis in the mouse embryo. *Nature* **395**, 702-707.
Echarri, A., Lai, M. J., Robinson, M. R. and Pendergast, A. M. (2004). Abl interactor 1 (Abi-1) wave-binding and SNARE domains regulate its nucleocytoplasmic shuttling, lamellipodium localization, and Wave-1 levels. *Mol. Cell. Biol.* **24**, 4979-4993.
Eden, S., Rohatgi, R., Podtelejnikov, A. V., Mann, M. and Kirschner, M. W. (2002). Mechanism of regulation of WAVE1-induced actin nucleation by Rac1 and Nck. *Nature* **418**, 790-793.
Eggenschwiler, J. T. and Anderson, K. V. (2000). Dorsal and lateral fates in the mouse neural tube require the cell-autonomous activity of the *open brain* gene. *Dev. Biol.* **227**, 648-660.
García-García, M. J., Eggenschwiler, J. T., Caspary, T., Alcorn, H. L., Wyler, M. R., Huangfu, D., Rakeman, A. S., Lee, J. D., Feinberg, E. H., Timmer, J. R. et al. (2005). Analysis of mouse embryonic patterning and morphogenesis by forward genetics. *Proc. Natl. Acad. Sci. USA* **102**, 5913-5919.
Gautreau, A., Ho, H. Y., Li, J., Steen, H., Gygi, S. P. and Kirschner, M. W. (2004). Purification and architecture of the ubiquitous Wave complex. *Proc. Natl. Acad. Sci. USA* **101**, 4379-4383.
Grove, M., Demyanenko, G., Echarri, A., Zipfel, P. A., Quiroz, M. E., Rodriguiz, R. M., Playford, M., Martensen, S. A., Robinson, M. R., Wetsel, W. C. et al. (2004). ABI2-deficient mice exhibit defective cell migration, aberrant dendritic spine morphogenesis, and deficits in learning and memory. *Mol. Cell. Biol.* **24**, 10905-10922.
Hummel, T., Leifker, K. and Klämbt, C. (2000). The *Drosophila* HEM-2/NAP1 homolog KETTE controls axonal pathfinding and cytoskeletal organization. *Genes Dev.* **14**, 863-873.
Ibarra, N., Blagg, S. L., Vazquez, F. and Insall, R. H. (2006). Nap1 regulates *Dictyostelium* cell motility and adhesion through SCAR-dependent and –independent pathways. *Curr. Biol.* **16**, 717-722.
Innocenti, M., Zucconi, A., Disanza, A., Frittoli, E., Areces, L. B., Steffen, A., Stradal, T. E., Di Fiore, P. P., Carlier, M. F. and Scita, G. (2004). Abi1 is essential for the formation and activation of a WAVE2 signalling complex. *Nat. Cell Biol.* **6**, 319-327.
Kimura-Yoshida, C., Nakano, H., Okamura, D., Nakao, K., Yonemura, S., Belo, J. A., Aizawa, S., Matsui, Y. and Matsuo, I. (2005). Canonical Wnt signaling and its antagonist regulate anterior-posterior axis polarization by guiding cell migration in mouse visceral endoderm. *Dev. Cell* **9**, 639-650.
Kinder, S. J., Tsang, T. E., Ang, S. L., Behringer, R. R. and Tam, P. P. (2001). Defects of the body plan of mutant embryos lacking *Lim1*, *Otx2* or *Hnf3beta* activity. *Int. J. Dev. Biol.* **45**, 347-355.
Kitamura, T., Kitamura, Y., Yonezawa, K., Totty, N. F., Gout, I., Hara, K., Waterfield, M. D., Sakaue, M., Ogawa, W. and Kasuga, M. (1996). Molecular cloning of $p125^{Nap1}$, a protein that associates with an SH3 domain of Nck. *Biochem. Biophys. Res. Commun.* **219**, 509-514.
Kobayashi, K., Kuroda, S., Fukata, M., Nakamura, T., Nagase, T., Nomura, N., Matsuura, Y., Yoshida-Kubomura, N., Iwamatsu, A. and Kaibuchi, K. (1998). p140Sra-1 (specifically Rac1-associated protein) is a novel specific target for Rac1 small GTPase. *J. Biol. Chem.* **273**, 291-295.
Koleske, A. J., Gifford, A. M., Scott, M. L., Nee, M., Bronson, R. T., Miczek, K. A. and Baltimore, D. (1998). Essential roles for the Abl and Arg tyrosine kinases in neurulation. *Neuron* **21**, 1259-1272.
Liu, P., Wakamiya, M., Shea, M. J., Albrecht, U., Behringer, R. R. and Bradley, A. (1999). Requirement for *Wnt3* in vertebrate axis formation. *Nat. Genet.* **22**, 361-365.
Lu, C. C., Brennan, J. and Robertson, E. J. (2001). From fertilization to gastrulation: axis formation in the mouse embryo. *Curr. Opin. Genet. Dev.* **11**, 384-392.
Merrill, B. J., Pasolli, H. A., Polak, L., Rendl, M., García-García, M. J., Anderson, K. V. and Fuchs, E. (2004). Tcf3: a transcriptional regulator of axis induction in the early embryo. *Development* **131**, 263-274.
Meyers, E. N., Lewandoski, M. and Martin, G. R. (1998). An *Fgf8* mutant allelic series generated by Cre- and Flp-mediated recombination. *Nat. Genet.* **18**, 136-141.
Perea-Gomez, A., Lawson, K. A., Rhinn, M., Zakin, L., Brûlet, P., Mazan, S. and Ang, S. L. (2001). Otx2 is required for visceral endoderm movement and for the restriction of posterior signals in the epiblast of the mouse embryo. *Development* **128**, 753-765.
Pöpperl, H., Schmidt, C., Wilson, V., Hume, C. R., Dodd, J., Krumlauf, R. and Beddington, R. S. (1997). Misexpression of *Cwnt8C* in the mouse induces an ectopic embryonic axis and causes a truncation of the anterior neuroectoderm. *Development* **124**, 2997-3005.
Rivera-Pérez, J. A. and Magnuson, T. (2005). Primitive streak formation in mice is preceded by localized activation of *Brachyury* and *Wnt3*. *Dev. Biol.* **288**, 363-371.
Rodriguez, T. A., Srinivas, S., Clements, M. P., Smith, J. C. and Beddington, R. S. (2005). Induction and migration of the anterior visceral endoderm is regulated by the extra-embryonic ectoderm. *Development* **132**, 2513-2520.
Roebroek, A. J., Umans, L., Pauli, I. G., Robertson, E. J., van Leuven, F., Van de Ven, W. J. and Constam, D. B. (1998). Failure of ventral closure and axial rotation in embryos lacking the proprotein convertase Furin. *Development* **125**, 4863-4876.
Shawlot, W. and Behringer, R. R. (1995). Requirement for *Lim1* in head-organizer function. *Nature* **374**, 425-430.
Shawlot, W., Deng, J. M. and Behringer, R. R. (1998). Expression of the mouse *cerberus*-related gene, *Cerr1*, suggests a role in anterior neural induction and somitogenesis. *Proc. Natl. Acad. Sci. USA* **95**, 6198-6203.
Soderling, S. H., Langeberg, L. K., Soderling, J. A., Davee, S. M., Simerly, R., Raber, J. and Scott, J. D. (2003). Loss of WAVE-1 causes sensorimotor retardation and reduced learning and memory in mice. *Proc. Natl. Acad. Sci. USA* **100**, 1723-1728.
Soto, M. C., Qadota, H., Kasuya, K., Inoue, M., Tsuboi, D., Mello, C. C. and Kaibuchi, K. (2002). The GEX-2 and GEX-3 proteins are required for tissue morphogenesis and cell migrations in *C. elegans*. *Genes Dev.* **16**, 620-632.
Srinivas, S., Rodriguez, T., Clements, M., Smith, J. C. and Beddington, R. S. (2004). Active cell migration drives the unilateral movements of the anterior visceral endoderm. *Development* **131**, 1157-1164.
Steffen, A., Rottner, K., Ehinger, J., Innocenti, M., Scita, G., Wehland, J. and Stradal, T. E. (2004). Sra-1 and Nap1 link Rac to actin assembly driving lamellipodia formation. *EMBO J.* **23**, 749-759.
Stryke, D., Kawamoto, M., Huang, C. C., Johns, S. J., King, L. A., Harper, C. A., Meng, E. C., Lee, R. E., Yee, A., L'Italien, L. et al. (2003). BayGenomics: a resource of insertional mutations in mouse embryonic stem cells. *Nucleic Acids Res.* **31**, 278-281.
Sugihara, K., Nakatsuji, N., Nakamura, K., Nakao, K., Hashimoto, R., Otani, H., Sakagami, H., Kondo, H., Nozawa, S., Aiba, A. et al. (1998). Rac1 is required for the formation of three germ layers during gastrulation. *Oncogene* **17**, 3427-3433.
Takaoka, K., Yamamoto, M., Shiratori, H., Meno, C., Rossant, J., Saijoh, Y. and Hamada, H. (2006). The mouse embryo autonomously acquires anterior-posterior polarity at implantation. *Dev. Cell* **10**, 451-459.
Tam, P. P. and Behringer, R. R. (1997). Mouse gastrulation: the formation of a mammalian body plan. *Mech. Dev.* **68**, 3-25.
Tam, P. P., Gad, J. M., Kinder, S. J., Tsang, T. E. and Behringer, R. R. (2001). Morphogenetic tissue movement and the establishment of body plan during development from blastocyst to gastrula in the mouse. *BioEssays* **23**, 508-517.
Thomas, P. Q., Brown, A. and Beddington, R. S. (1998). *Hex*: a homeobox gene revealing peri-implantation asymmetry in the mouse embryo and an early transient marker of endothelial cell precursors. *Development* **125**, 85-94.
Weed, S. A., Karginov, A. V., Schafer, D. A., Weaver, A. M., Kinley, A. W., Cooper, J. A. and Parsons, J. T. (2000). Cortactin localization to sites of actin assembly in lamellipodia requires interactions with F-actin and the Arp2/3 complex. *J. Cell Biol.* **151**, 29-40.
Weiner, O. D., Rentel, M. C., Ott, A., Brown, G. E., Jedrychowski, M., Yaffe, M. B., Gygi, S. P., Cantley, L. C., Bourne, H. R. and Kirschner, M. W. (2006). Hem-1 complexes are essential for Rac activation, actin polymerization, and myosin regulation during neutrophil chemotaxis. *PLoS Biol.* **4**, e38.
Xue, Y., Wang, X., Li, Z., Gotoh, N., Chapman, D. and Skolnik, E. Y. (2001). Mesodermal patterning defect in mice lacking the Ste20 NCK interacting kinase (NIK). *Development* **128**, 1559-1572.
Yamamoto, M., Saijoh, Y., Perea-Gomez, A., Shawlot, W., Behringer, R. R., Ang, S. L., Hamada, H. and Meno, C. (2004). Nodal antagonists regulate formation of the anteroposterior axis of the mouse embryo. *Nature* **428**, 387-392.
Yamazaki, D., Suetsugu, S., Miki, H., Kataoka, Y., Nishikawa, S., Fujiwara, T., Yoshida, N. and Takenawa, T. (2003). WAVE2 is required for directed cell migration and cardiovascular development. *Nature* **424**, 452-456.
Yan, C., Martinez-Quiles, N., Eden, S., Shibata, T., Takeshima, F., Shinkura, R., Fujiwara, Y., Bronson, R., Snapper, S. B., Kirschner, M. W. et al. (2003). WAVE2 deficiency reveals distinct roles in embryogenesis and Rac-mediated actin-based motility. *EMBO J.* **22**, 3602-3612.